

Semi-Autonomous Control of A Multi-Agent Robotic System for Multi-Target Operations

Yushing Cheung

*Department of Mechanical Engineering,
Stevens Institute of Technology,
Hoboken, NJ 07030, USA*

ycheung@stevens.edu

Jae H. Chung

*US Army RDECOM-ARDEC,
Building 95N,
Picatinny Arsenal, NJ 07806, USA*

jchung3@stevens.edu

Abstract

Since multi-targets often occur in most applications, it is required that multi-robots are grouped to work on multi-targets simultaneously. Therefore, this paper proposes a control method for a single-master multi-slave (SMMS) teleoperator to control cooperative mobile multi-robots for a multi-target mission. The major components of the proposed control method are the robot-target pairing method and modified potential field based leader-follower formation.

The robot-target paring method is derived from the proven auction algorithm for a single target and is extended for multi-robot multi-target cases, which optimizes effect-based robot-target pairing based on heuristic and sensory data. The multi-robot multi-target pairing method can produce a weighted attack guidance table (WAGT), which contains benefits of different robot-target pairs. The robot-target pairing converges rapidly - as is the case for auction algorithms with integer benefits.

Besides, as long as optimal robot-target pairs are obtained, a team is split into subteams formed by paired robots regarding types and numbers of the robot-target pairs with the robot-target pairing method. The subteams approach and then capture their own paired targets in the modified potential field based leader-follower formation while avoiding sensed obstacles.

Simulation studies illustrate system efficacy with the proposed control method for multi-target operations. Moreover, the paper is concluded with observations of enhanced system performance.

Keywords: Teleoperation, Multi-target Operations, and Multi-agent Systems.

1. INTRODUCTION

Cooperative control of multi-agent robotic systems has been investigated in recent years [36, 47], especially for tasks that cannot be handled by a single robot. It can improve dexterity of robots and enlarge application fields of robots. Furthermore, Fox et. al. [19] have demonstrated that multi-robots can localize themselves faster and more accurately if they exchange information about their positions whenever they sense each other. Moreover, using several low-cost robots introduces redundancy and therefore is more fault tolerant than having only one powerful and expensive robot. Therefore, there have been many cooperative control methods, e.g. the behavior based formation control, virtual structure approach, leader-follower approach, and potential field based control method for multi-robot navigation and searching [2,12,26,29,42,43].

Balch and Arkin [2] presented behavior based formation control. The temporary distortion in a formation was used to avoid obstacles. However, the system is not able to be analyzed in terms of simple mathematic equations. Therefore, exact formation control of the system cannot be guaranteed. Lalish et. al. [26] suggested the virtual structure approach by considering the robot

formation as a single virtual rigid structure. The behavior of the whole group is totally predictable, and its formation is precisely maintained. However, a wider inter-robot communication is necessary, which causes more communication delays. Desai et. al. [12] proposed a leader-follower approach. One or more robots are designated as the leader(s) and responsible for guiding the formation. The other robots are required to follow the leader(s) with predefined clearances. This leader-follower approach has some benefits, e.g. its simplicity, modularity, and reliability of the system and no need for heavy computation. However, the whole team is potentially subjected to system malfunctions if the leader(s) break(s) down. In addition, there is a risk that the followers get too close to each other while only keeping a constant leader-follower distance without considering the follower-follower distances. Due to no interconnection between the followers, the follower cannot distinguish between its team robots and obstacles. Therefore, if the robot-robot distance that the robot needs to maintain in the team is different from the robot-obstacle distance that the robot needs to keep from the obstacles, the follower may hit the other robot or obstacle. Artificial potential functions have been extensively used for multi-robot navigation and control [3,8,14,20,29,41,44]. The robots are attracted to the target while being repulsed from the obstacles as if the robots and obstacles as positive ions and the target as a negative ion were in potential fields.

By comparing those above mentioned approaches, the potential function based approaches seemed to be useful tools from the view points of flexibility of configurations of robotic teams, automatic avoidance of collisions of team robots, and stability of maintaining formations. However, the multiple fields can sum to a vector with a zero magnitude. If the robot was being attracted to a point behind the box canyon, the attractive vector would cancel the repulsive vector and the robot would remain stationary because all forces would cancel out. This is called a local minima problem [2,21,29,38,48].

Besides, all control methods discussed above for the robot cooperation are only for the fully autonomous robots. Nonetheless, the unstructured nature of the worksite environments and the limitations of the current sensors and computer decision-making technologies prohibit the use of fully autonomous systems for the operations [1,17,18,22,27,28,37]. Therefore, it is required that the human decision making be involved in the systems. Teleoperators, in which a human operator is an integral part of the control, are established to integrate the human decisions to the control loop of the systems. In order to minimize the required human resources and amplify the human effort, a single-master multi-slave (SMMS) teleoperation is considered in this paper [17,18, 22, 27, 28, 33,37].

Nevertheless, that a teleoperated robot may be of varying types with varying capabilities and limitations places significant cognitive pressure on the operator. As has been demonstrated in urban search and rescue activities [19], simply remotely operating a robotic system in a challenging environment precludes significant secondary cognitive effort (such as scanning rubble for survivors). The difficulties will be compounded when the human operator remotely guides multiple robots in a rapidly evolving operational environment. Therefore, it is required that some local robotic intelligence is added to the SMMS teleoperator to relieve human burden and enhance the performance. Nonetheless, so far a few papers have discussed the semi-autonomous SMMS teleoperation issues. Moreover, most of them were only focused on a single target operation.

However, most applications [45,46] e.g. military operation, space exploration, rescue mission, and etc, require a team of robots to form several subteams to capture multi-targets simultaneously. Therefore, the robot-target pairing method is needed to identify a proper target that can be captured by a suitable subteam of robots. Many different methods have been widely applied in fully automatic coordinated multi-robotic systems [9,11,15,30,32,35,39]. Those methods are a genetic or improved genetic [9,10,16,34], ant colony system [15,30], swarm particle optimization (SPO) [11,32], market-based approaches [13,23,24,31], and auction or decentralized cooperation auction [25,35,39]. Nonetheless, some of them [9,30,32] can have a slow convergence to the global optimum when the others [13,39] have no ability to stably

converge to a global optimum. Hence, Bogdanowicz and Coleman et. al. [4] proposed a pairing method for optimization of effect-based weapon-target pairing to decide a preferred weapon-target combination by scanning a heuristic attack guidance table. Different from those previously mentioned methods, it is a rule and function based method. Therefore, it can converge rapidly and produce a suboptimal solution stably. Nonetheless, it is derived based on some heuristic data that come from human experiences.

Due to the above mentioned problems, in this paper, the primary objective is to develop a control method for a SMMS teleoperation system to cooperatively control mobile multi-robots for a multi-target mission. Primary components of the proposed method are (1) modified potential field based leader-follower formation and (2) robot-target pairings. During the operation, the human operator only concentrates on teleoperating a team leader robot. All other team robots autonomously make a formation with regard to its positions and velocities based on sensory information. Therefore, the formation is able to be adapted by modifying their paths for obstacle avoidance and target pursuit in the modified potential field based leader-follower formation. As soon as the team is near the multi-targets, with the proposed robot-target pairing method, optimal robot-target pairs are computed, and according to them, the team is autonomously split into several subteams that are paired to appropriate targets. A subteam leader is selected based on all robot functionalities and proximity to targets to lead each subteam. Each subteam leader is able to guide all subteam robots to work on the paired targets when the subteam robots move with respect its motion.

The rest of this paper is organized as follows. In Section 2, the control method that integrates the primary components to capture multiple targets simultaneously with multiple subteams independently for is proposed. This system with the proposed control method is aimed at relieving human operator burden of teleoperating a robot team that is formed by several sub-teams in a complex environment to handle multi-targets simultaneously. In Section 3, the conditional transparency [5], i.e. the transparency if no human induced error is found, and effectiveness of the task achievement of the SMMS teleoperation system with the proposed control method were evaluated through simulation studies. Section 4 concludes this paper and shows future research directions.

2. SEMI-AUTONOMOUS TELEOPERATION CONTROL METHOD FOR A MULTI-ROBOTS-MULTI-TARGETS APPROACH

This paper proposes a control method for the semi-autonomous SMMS teleoperation to work on a multi-target mission. The major components of the control method are (1) modified potential field based leader-follower formation and (2) robot-target pairings. They are described in details in the following. During robot navigation to targets, a team/subteam moves in (1) modified potential field based leader-follower formation. Nonetheless, as long as the team is close enough to the targets, it will be split into subteams that are paired to suitable targets with (2) robot-target pairing method. Therefore, in the following, the two components are discussed and formulated in detail.

2.1 Modified Potential Field Based Leader-follower Formation

In order that the slave multi-robots can autonomously avoid the obstacles and keep a distance from other neighboring robots simultaneously while tracking the target, the approach that the most commonly has been used is potential field based formation control. Nonetheless, the potential field based formation control has the local minima problem [29], which can hold the robots in a specified formation while in motion. Therefore, the potential field based formation is modified into the one with a prioritized bonding between slave neighboring robots in this paper. The strength of the bonding between neighboring robots varies depending on which two robots are connected.

For example, the bonding between neighboring team/subteam *Leader* and *Follower*–1 is the strongest when the one between team/subteam *Follower*–*n* and *Leader* is the weakest if there are *n* robots. Furthermore, as soon as the subteam is formed, only bonding between subteam

robots exists when the subteam followers move only with regard to their subteam leader. Thus, the team/subteam formation becomes adaptive due to attraction to targets and repulsion from obstacles. However, no team/subteam robot is left behind due to the robot-robot bonding with different strengths, and no subteam robot movement is affected by other subteam/team robot motion because of the elimination of the bonding between the subteam and irrelevant robots.

Besides, the team leader tracks the human commanded positions when the subteam leaders follow the reference positions to capture the targets and avoid obstacles and neighboring robots. In the potential field based leader-follower formation, all team/subteam follower paths are generated by a sum of attraction, repulsion, and prioritized bonding. All team/subteam leader paths are computed by a combination of the attraction and repulsion. In our discussion, we assume that for Robot i , the control input, u_i^i generated by using the potential field based leader-follower formation method are typically of the form.

$$u_i^i = u_a^i + u_r^i + u_b^i \quad (1)$$

where for Robot i , u_a^i is the control input caused by the attraction to the targets. u_r^i is the control input caused by the repulsion from the obstacles. u_b^i is the control input caused by the robot-robot bonding for the team/subteam followers. u_b^i can become zero for the team/subteam leaders. In the following, the control inputs due to (1) the attraction to the targets, (2) repulsion from the obstacles, and (3) bonding between robots are formulated and discussed.

2.1.1 Attraction to Targets

The control input u_a^i in Eq (1) derived from the target potential functions for the robot is formulated in Eq. (2).

$$u_a^i = \varphi_i \delta x_T \quad (2)$$

where δx_T is the sensed distance between Robot i and the paired target. Robot i can be any robot in a team or subteam. φ_i is a positive integer that becomes zero if the target is reached; otherwise, it is larger than zero. As shown in Eq. (2), if Robot i is getting closer to the paired target, u_a^i is decreased. On the contrary, if it is leaving the paired target, u_a^i is increased. Therefore, it is attracted to the paired target all the time.

2.1.2 Repulsion from Obstacles

The control input u_r^i in Eq (1) derived from the obstacle potential functions is written in Eq. (3).

$$u_r^i = \phi \langle -k_e \delta D_1 - b_e \delta V_1 \rangle \quad (3)$$

where for Robot i , $\delta V_1 = -\frac{G}{\delta x_0^2} \dot{x}_{si}$, and $\delta D_1 = -\frac{H}{\delta x_0^2}$. δx_o is the sensed robot-obstacle distance. x_{si} is the position vector of Robot i . ϕ , G , H , k_e , and b_e are positive parameters. In Eq (3), u_r^i is increased when Robot i is heading toward obstacles. On the contrary, u_r^i is decreased when it is steering away from the obstacles. Thus, it is repulsed from the obstacles all the time.

2.1.3 Bonding Between Robots

For team/subteam followers, the robot-robot bonding u_b^i in Eq. (1) is prioritized regarding the roles of the neighboring robots and formulated in the following equation.

$$u_b^i = -k_{ij}(r_{s \min i} - \delta x_{si}) \quad (4)$$

where for $i = 1, \dots, n$ and $j = 1, \dots, n$, $i \neq j$, k_{ij} is the positive parameter. The bonding strength varies because of different roles of the neighboring robots bonding to each other. $r_{s \min i}$ is the preferred distance that Robot i needs to keep from neighboring robots. δx_{si} is the sensed distance between Robot i and other robots. Therefore, the team/subteam followers move with regard to their team/subteam leader motion while keeping a predefined constant distance from team/subteam leader with Eq. (4). All team/subteam robots can also get around the obstacles with Eq. (3) and move toward the targets with Eq. (2).

2.2 Robot-target Pairing Method

The robot-target pairing method is sensor based and semi-distributed because all robots act largely independently in terms of planning for themselves but are able to take into account team resources by working on the tasks with other robots. It is more flexible than the centralized robot-target pairing method [9,30,32] in that each individual robot can respond to different environment stimulus independently relying on its local sensory information. In addition, it is also more robust and reliable than the distributed robot-target pairing method [13,39] in that each robot also can take advantage of sharing team resources to work with other team robots. In this paper, the team leader not only takes human commands via a master robot but also works with the robot-target pairing method as an auctioneer to send and show all bid data e.g. robot-target distances and their base prices. The bid data are also online shared by all robots, team leader and followers. All other robots, e.g. team followers, act as bidders to form a subteam by themselves in order to maximize a sum of all follower bid values and bid on the targets when the corresponding task on the targets is performed by the cooperation of the subteam. In the subteam, the bidder with the maximum bid value is selected as a subteam leader. The subteam leader is responsible for monitoring and coordinating all subteam member actions. According to the largest bid proposed by the subteam, the auctioneer, the team leader, decides which subteam wins the bid with a restriction that only one target is gained by every subteam per auction. If all subteam bid values are smaller than the base price, or any team robot cannot compute its bid value due to insufficient sensed data surrounding the targets, the auctioneer obtains the bid. If any subteam already completes the task on the target, it will inform the auctioneer to cancel the bid. The proposed robot-target pairing method is formulated and further discussed in the following.

2.2.1 Robot-target Pairing Formulation and Discussion

Consider such a scenario, in a two-dimensional and limited rectangular environment X with n_c square cells, n_p slave robots pursue n_e targets, for $n_p > n_e$. The set of the robots is denoted by a matrix of $A = [a_1 a_2 \dots a_{n_p}]$ where a_{n_p} is a robot matrix of n_p . Robot Capability Vector j for Task t is denoted by \hat{C}_j^t , $1 \leq j \leq n_p$ and the set of targets is represented by a target matrix of $T = [T_1 T_2 \dots T_{n_e}]$ where T_{n_e} is a target matrix of n_e . The vector representing the capability required to accomplish Task t on Target T is denoted by \bar{C}_t^T , $1 \leq t \leq n_e$. Agent $A \cup T$ denotes robot teams and targets. For simplification, we assume that both space and time can be quantized, therefore the environment can be regarded as a finite collection of cells, denoted by $X_c = [1, 2, \dots, n_c]$. There exist some static obstacles with fixed sizes and regular shapes, and their locations are determined by the mapping $m : X_c \rightarrow 0, 1$, for $\forall x \in X_c, M(x) \geq thresh1$ indicates

that the cell x is occupied by obstacles. $\forall x \in X_c, M(x) \leq \text{thresh2}$ indicates that the cell x is free, where $\text{thresh2} < \text{thresh1}$ represents the threshold value between 0 and 1. Thus, each robot has different capabilities to complete different tasks on different targets.

Robot capability - For Task t and Robot j , the weighted capability vectors of Robot j can be defined as

$$\hat{C}_j^t = w_j^T \text{diag}\{b_{j1}^t b_{j2}^t \dots b_{ju}^t\} [c_{j1}^t \dots c_{ju}^t]^T \quad (5)$$

where u is the maximum number of the vectors, each of which represents the individual functionality. The set of robot matrices is rewritten into $A = \begin{bmatrix} a_{11} \dots a_{1r} \\ a_{21} \dots a_{2r} \\ \dots \\ a_{n_r 1} \dots a_{n_r r} \end{bmatrix}$ where n_v , for $0 < n_v \leq n_p$,

is the total number of the robots in the team, and r , for $0 < r \leq n_e$ is the total number of the tasks. c_{jk}^t is a capability vector for Functionality k and Task t . w_j^T is a positive integer such that for Target T and Robot j , the following is satisfied. If the robot is assigned to the target, $w_j^T = 0$; otherwise, $w_j^T = 1$. The $u \times u$ dimension diagonal matrix of b_{ju}^t is used to estimate the percentage of possibility of using the $u \times 1$ dimensional capability vector C_j^t to do Task t by Robot j successfully. However, if Robot j does not have Capability c_{jk}^t , then b_{ju}^t is 0. Each robot matrix in A has weighted capability vectors, e.g. for Robot j and Task t , $a_{jt} = [\hat{C}_j^t]^T$.

Capability Required Executing Tasks on Targets

It is assumed that one target can be paired to two or more robots, but one robot can only be paired to one target. The capability vector that is required to accomplish Task t on Target T is defined as

$$\bar{C}_t^T = \text{diag}\{\beta_{t1}^T \dots \beta_{tu}^T\} C_{tu} \quad (6)$$

where the $u \times u$ dimension diagonal matrix of β_{tu}^T is used to describe the percentage of possibility of using the $u \times 1$ dimension capability vector C_{tu} with which the robot can finish Task t on Target T . $C_{tu} = [c_{t1} \dots c_{tu}]^T$ when the total number of the vectors of the functionalities is u . c_{tu} is the capability vector that is required to complete Task t with Functionality u . However, if Task t cannot be done successfully by any robot with the capability C_{tu} on Target T , then β_{tu}^T is 0. Otherwise, β_{tu}^T is 1.

Subteam Capability

The subteam is a combination of the multi-robots that work on Task t cooperatively. For Robot j and Task t , $U_{(j,t)} = a_j e_t$ where e_t is one if Task t is assigned; otherwise, it is zero, and a_j is defined in Eq. (1) for $a_{\max} \geq j \geq a_{\min}$, $a_{\min} \geq 1$, and $a_{\max} \leq n_p$ where $n_p / (a_{\max} - a_{\min} + 1) = n_s$ where n_s is the total number of subteams, and a_{\max} and a_{\min} are the

number of the first and last robots forming Subteam y , respectively. Subteam y is represented

by a matrix of $D_y = \begin{bmatrix} U_{(a_{\min},1)} \dots U_{(a_{\max},1)} \\ \dots \\ U_{(a_{\min},r)} \dots U_{(a_{\max},r)} \end{bmatrix}$ where r is the total number of tasks. Then, matrix

A denoting a robot team formed by subteams, one of which is represented by D_y , is rewritten into $A = \{D_1, \dots, D_y, \dots, D_q\}$ where q is the total number of the combinations of multi-robots (robot subteams) in the team. For Robot j and Task t , if $\hat{C}_j^t > 0$, then

$$Q_{(j,t)} = \hat{C}_j^t \quad \text{for } n_p \geq j \geq 1 \quad (7)$$

where $Q = \{Q_{(1,t)}, \dots, Q_{(n_p,t)}\}$ is a positive integer. Subteam y capability vector for Task t is defined as

$$\tilde{C}_{(y_a:y_b,t)}^y = \sum_{j=y_b}^{j=y_a} Q_{(j,t)} \quad (8)$$

where $y_b - y_a$, $\forall y_b \geq y_a$, is the total number of the robots in Subteam y . y_a is the first and y_b is the last indices of the elements in the matrix of Q for Task t and Subteam y . Subteam y is able to perform Task t on Target T if the condition, $\bar{C}_t^T \leq \tilde{C}_{(y_a:y_b,t)}^y$, is satisfied. Robot j is selected as a subteam leader when its magnitude of the capability vector \hat{C}_j^t is largest in the same subteam. It is assumed that the subteam leader knows all capability information about its subteam members.

2.2.2 Bidding Winner Determination

Subteam 1	$m_{N,1}$	\dots	Subteam n	$m_{N,n}$
B_1^1	$m_{1,1}$	\dots	B_n^1	$m_{1,n}$
B_1^2	$m_{2,1}$	\dots	B_n^2	$m_{2,n}$
\dots	\dots	\dots	\dots	\dots
B_1^N	$m_{N,1}$	\dots	B_n^N	$m_{N,n}$

TABLE 1: Weighted Attack Guidance Table (WAGT)

In Table 1, $m_{N,n}$ is a positive integer weight for Subteam n to bid on Target N . If $\tilde{C}_{(y_a:y_b,N)}^n$ is smaller than the base price which is a positive integer, or Target N has already been assigned to Robot Subteam n , $m_{N,n}$ is 0. Otherwise, $m_{N,n}$ is 1. By arranging $m_{N,n}$ and B_n^N into Table 1, called Weighted Attack Guidance Table (WAGT), each row of WAGT corresponds to a target and Robot Subteam (1 to n) when n is the total number of the subteams formed in the team. In addition, each column of WAGT corresponds to a robot combination (Robot Subteam) that works on Targets (1 to N) when N is the total number of the targets. Therefore, there are the N rows and n columns in WAGT. The scanning proceeds from the first to the last column. Hence, the robot combination (Robot Subteam) specified in column i takes precedence over combination of

robots specified in column $i+1$. For example, for Subteam n , Task t , and Target N , the bid value is weighted as follows.

$$B_n^N = (\tilde{C}_{(y_a:y_b,t)}^n - \bar{C}_t^N)(1 - X_{tm}^N) \quad (9)$$

where X_{tm}^N is the positive integer weight for Subteam n to do Target N . If Task t is the most preferred by Subteam n to be done on Target N when B_n^N is the maximum value of the element in the matrix of $\tilde{B}(N,n)$, then $X_{tm}^N = 0$. Otherwise, $X_{tm}^N = 1$. Therefore, based on the given subteams, targets, tasks, WAGT, and optimization of the robot-target pairing that is described below, the bidding winner determination is made.

The optimization of the robot-target pairing is formulated as follows. Given Subteam y , Targets N , Tasks t , and WAGT, an assignment of the subteam is found in such a format that WAGT is produced, and its corresponding objective function in Eq.(10) is maximized within the given constraints in Eqs. (11) and (12). Therefore, we can state the optimization problem as follows. For Target N and Subteam $1-n$ as seen in Table 1, the objective function is $ObjFun(N) = [(B_1^N m_{N,1}) \dots (B_n^N m_{N,n})]$.

$$\text{Maximize} \quad ObjFun(N) \quad (10)$$

Subject to

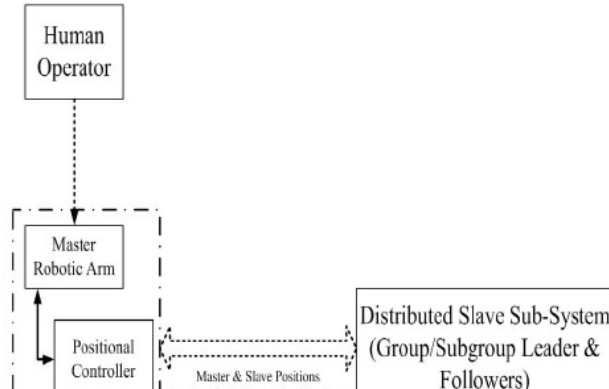
$$\sum_{y=1}^{y=n} m_{N,y} \geq 0 \quad (11)$$

$$\sum_{y=1}^{y=n} \tilde{B}(N, y) \geq 0 \quad (12)$$

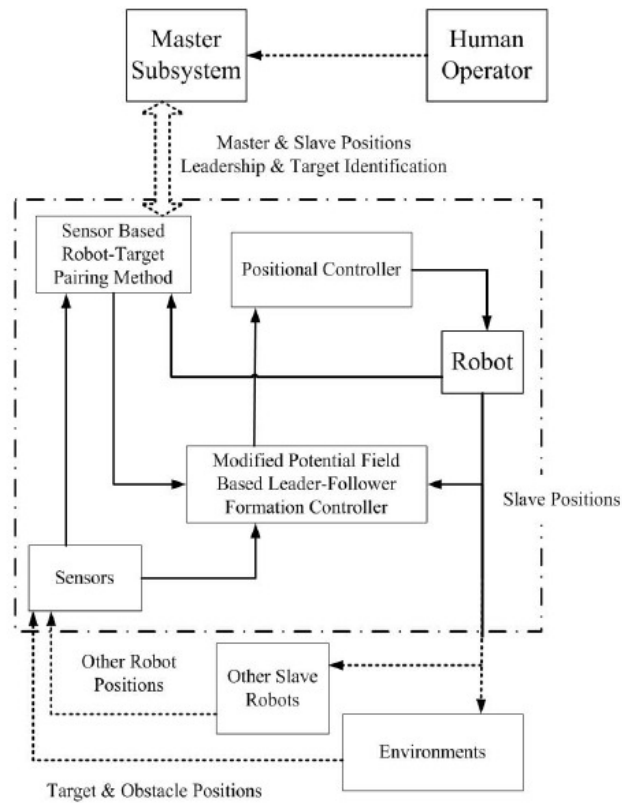
where $m_{N,y}$ is defined in Table 1. Initially, all $m_{N,y}$ is equal to one if no subteam is assigned to any target. However, if Subteam y is assigned to Target N , $m_{N,y}$ is equal to zero $\forall y \& N \neq 0$. Hence, Subteam y that proposes the maximum affordable value ($B_y^N m_{N,y}$) can win Target N by solving Eqs (10) within the constraints Eqs. (11) and (12). By using the proposed robot-target pairing method, the robot-target pairs are stored into the resulted matrix e.g. a subteam-target pair matrix J_I and given WAGT. For instances, Subteam y is paired to Target N when Subteam $(y+1)$ is paired to Target $N+1$. The subteam-target pair matrix, J_I is written as $J_I = [.., N, N+1]$ when the first and second columns of the J_I represent which target is properly paired to Subteam y and $y+1$, respectively. In order to make the system be able to split its team into subteams to work on different targets simultaneously, the robot-target pairing method can also generate reference positions X_r to each subteam robot to move toward its target point by transforming J_I based on WAGT.

2.3 SMMS Teleoperator With Modified Potential Field Based Leader-follower Formation and Robot-target Pairing Methods

Figure 1 represents the overall architecture of the SMMS teleoperation system with the proposed control methods. The master and slave subsystems in Figures 1(a) and 1(b), respectively, are connected over the wireless internet. The difference from the system proposed in our papers [5] is that the slave subteam is operated fully autonomously with the modified potential field based leader-follower formation method when the team leader is teleoperated by a human operator.



(a) Master subsystem

**FIGURE 1:** Modified SMMS system

In order to simplify a problem, the robot is not supposed to move so fast that the nonlinear coefficients of the robotic dynamic equation can be ignored. The proposed system shown in Figure 1 can be formulated into the following equations of motion with integration of the modified potential field based leader-follower formation and robot-target pairing methods.

Master robot:

$$M_m \ddot{e}_m + B_m \dot{e}_m + K_m e_m = 0 \quad (13)$$

Slave robot i :

$$M_{si} \ddot{e}_{si} + B_{si} \dot{e}_{si} + K_{si} e_{si} = u_a^i + u_r^i + (1-\sigma)(1-\lambda)u_b^i \quad (14)$$

where for Robot i , u_a^i , u_r^i , and u_b^i are defined in Eq (1). $e_m = x_m - x_h$, x_h and x_m are the human commanded and master sensed position vectors, respectively. $e_{si} = x_{si} - (\alpha x'_m + (1-\sigma)x'_{ideal})x_h$, x_{si} is the position vector of the slave robot i . x'_m is the transmitted master position vector. x'_{ideal} is the reference position vector computed with respect to x'_m before a subteam is formed or X_r generated by transforming J_I resulting from Eqs (10)-(12) based on WAGT after the subteam is formed. σ is the control parameters of Robot i . When Robot i is selected as a team leader, σ is turned into one; otherwise, it becomes zero. When Robot i is appointed as a subteam leader, λ becomes one; otherwise, λ is zero. B_m is the master adaptive impedance matrix. M_m is the inertia matrix of the master robot. K_m is the control parameters for the linear diagonal master matrices. M_{si} is the inertia matrices of the slave robot i . B_{si} is the slave impedance matrix. K_{si} is the control parameters for the linear diagonal slave matrices.

By using Eqs. (13) and (14), the motion of the SMMS systems can be understood and modeled. The team moves toward a region full of multi-targets in the modified potential field based leader-follower formation when only team leader is teleoperated by the human operator via the master robot and followers autonomously move with regard to its motion. When the team is close to the targets, it can be split into subteams paired to targets with the robot-target pairing method by solving Eqs (10) within the constraints in Eqs (11) and (12). The robot-target matrix J_I is computed based on WAGT and transformed into the reference positions for the subteam robots to approach and capture the paired targets. During navigation to the paired targets, the subteams automatically move in the modified potential field based leader-follower formation again. In the formation, all subteam followers move with regard to their subteam leader's motion while the subteam leader approaches a target point computed from J_I . All subteam robots including the leader and followers can avoid obstacles while maintaining a formation. After the paired target is reached, a task, e.g. target capture, is performed by the paired subteam robots.

In the following section, the SMMS teleoperator modeled in Eqs (13) and (14) is simulated for a further study on enhancement of the performance in terms of conditional transparency [5] and task effectiveness.

3. SIMULATION STUDIES

In order to qualify and highlight the enhanced SMMS teleoperator performance, the scenario was that the SMMS system in Figure 2 with the one in [6,7] in Sim (1) and the proposed control methods in Sim (2) were properly simulated. Furthermore, Sim(1) and (2) were also subjected to the time-varying communication delay as shown in Figure 3. Results from Sim (1) and (2) are generated and compared to quantify and qualify the improvement of the performance in terms of conditional transparency [5] and task effectiveness. The simulation data from Sim (2) are discussed with findings from the research [9,13,32,39] to explicitly show advancement of convergence to an optimal solution to identify an appropriate subteam robot-target pair. The Sim (1) and (2) were set up in Table 2.

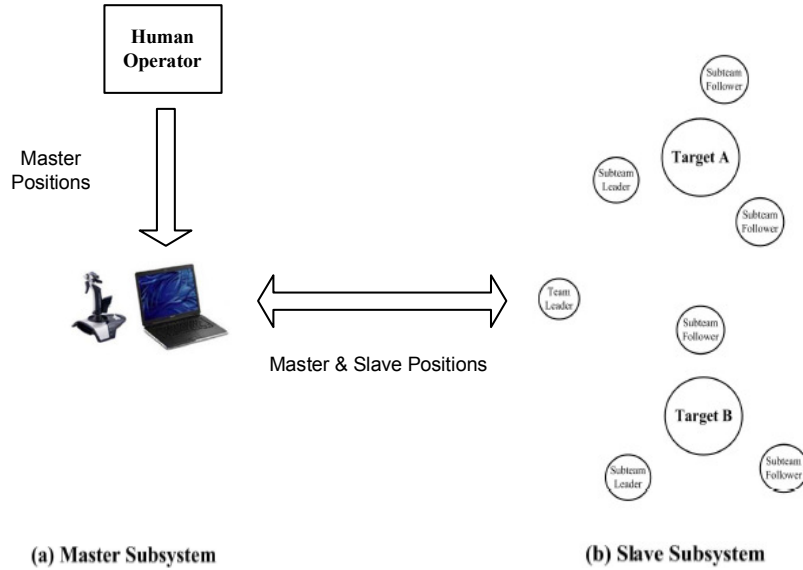


FIGURE 2: SMMS teleoperation simulation setup

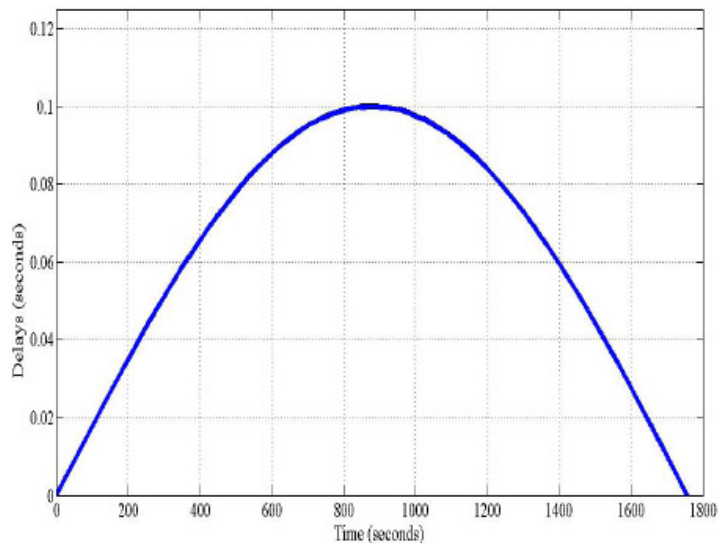


FIGURE 3: Time delays in simulations

Simulations	Control Methods	Control Objectives
Sim (1)	Positional control	adaptive leader-follower formation [7, 6]
Sim (2)	Positional control	potential field based leader-follower formation and proposed robot-target pairing

TABLE 2: SMMS simulations for a multi-target mission

In simulations, the time dependent communication delay was simulated in Figure 3. The maximum communication delay of 0.1 second was chosen in the simulations because for the earth application, there is a critical value, beyond which the system tends to become unstable

[40]. In the simulations, as shown in Figure 2, the master robot was a joystick connected to a laptop that read human operator motion commands. It was able to transmit human commands to a virtual slave robot model over the simulated TCP/IP internet. The virtual slave robots in Figure 2(b) including a team leader, subteam leaders, and followers were modeled in Matlab software and able to track the transmitted master and reference positions and velocities to execute the assigned tasks on the assigned targets. The slave robots also locally sensed the environments and then sent back the sensory information to the master robot. In the simulations, the slave robots were simulated as seven holonomic mobile platforms, each of which has two active wheels, and they formed a slave team. In addition, all of them did not have grippers. Moreover, there were six virtual static obstacles and two virtual targets in a virtual environment as shown in Figure 2. All target and robot positions were assumed to be known in the simulations, but obstacle positions were uncertain. The obstacles and targets were modeled as mass-spring-damper systems [40] in the following equations.

Targets:

$$M_T \ddot{x}_T + B_T \dot{x}_T + K_T x_T = F_T \quad (15)$$

Obstacles:

$$M_o \ddot{x}_o + B_o \dot{x}_o + K_o x_o = F_o \quad (16)$$

where M_T and M_o are the inertia matrices of the targets and obstacles, respectively. B_T and B_o are the damping coefficients of the targets and obstacles, respectively. K_T and K_o are the stiffness coefficients of the targets and obstacles, respectively. x_T and x_o are the position vectors of the targets and the obstacles, respectively. The seven slave robots were run to approach two targets, Target A (TA) and B (TB), while getting around the seven static obstacles. All targets, TA and TB, were static. The simple task, object capture, was performed by the slave robots simultaneously. Each of the targets was captured by at least three mobile robots. TA and TB were fixed on the ground. They were being captured while being encircled by the slave robots. The simulations, Sim (1) and Sim (2), as shown in Table 2, were set up with the following parameters. The desired safety distance between two robots was set to 3 m. The minimum distance between a robot and an obstacle was set to 5 m. Six circular objects with the radii of 5 m were used as obstacles in each simulation. In the simulations, the six circular obstacles, Ob1, Ob2, Ob3, Ob4, Ob5, and Ob6, were situated at (30, 60), (50, 40), (70, 20), (70,-20), (50,-40), and (30,-60), respectively. Another two circular objects with the radii of 5 m were also used as targets in each simulation. Two targets, TA and TB, were situated at (90, 30) and (90, -30), respectively, as shown in Figure 4 and 7. The seven slave robots, R1, 2, 3, 4, 5, 6, and 7, were initially located at (0, 15), (0, 10), (0, 5), (0, 0), (0, -5), (0, -10), and (0, -15), respectively. Only two directions parallel to the ground were considered in the simulations. Each slave robot was represented by a circular object with a radius of 1 m in the simulations. The master and slave positions were simulated in a computer with Matlab and divided by 10, respectively. In the simulations, the following parameters were used:

$$M_m = 3 \text{ kg}, \quad B_m = 6 \text{ Ns/m}, \quad K_m = 6 \text{ N/m}, \quad M_{si} = 30 \text{ kg}, \quad B_{si} = 1.0 \text{ Ns/m}, \quad K_{si} = 60 \text{ N/m}, \quad M_T = 60 \text{ kg}, \quad B_T = 0.0 \text{ Ns/m}, \quad K_T = 800 \text{ N/m}, \quad M_o = 6000 \text{ kg}, \quad B_o = 0.0 \text{ Ns/m}, \quad K_o = 1000 \text{ N/m}, \quad G = H = 1, \quad k_e = 100, \quad b_e = 60, \quad r_{i\min} = 5, \quad r_{s\min} = 5, \quad \varphi_i = \phi = 10000, \quad \text{and } k_{ij} = 50000(1/i + 1/j)$$

In the simulations, no friction, gravity, and air resistance were assumed in the virtual environment. The position errors are e_m and e_{si} . The simulations, Sim (1) and (2), as listed in Table 2 were conducted by the same human operator for consistency. All slave robots were programmed to move at an average speed of 0.1 m/s in the virtual environment in order to evaluate the effectiveness of the proposed systems by measuring the length of time taken to complete a task.

3.1 Simulation - Sim(1)

In Sim (1), the seven robots formed a team teleoperated by a human operator via the master robot. The human operator remotely controlled the team leader, R4, to reach TA, and all other slave robots, R1-3 and R5-7, were coordinated with R4 to surround TA to capture it. After the TA was captured, the human operator commanded R4 to move to TB while other robots, R1-3 and R5-7, were also moving with regard to R4 motion to approach TB. During the team navigations to catch TA and TB in Figure 4, all team robots were able to avoid the obstacles, Ob1-6, while they kept a constant distance from each other. As long as R4 was telecontrolled by the human operator to get to TB, R1-3 and R5-7 encircled and captured it.

In Figures 5 and 6, position errors e_{si} of the team leader and followers were presented, respectively. The position errors varied from 2.5 to 0 (m), which was caused by the time-varying communication delays. However, a position error average, 0.65 (m), was still acceptable because the team leader robot (R4) teleoperated by the human operator moved slowly when the follower robots (R1-3, 5-7) moved with regard to R4 positions. All targets were captured in 1350 seconds.

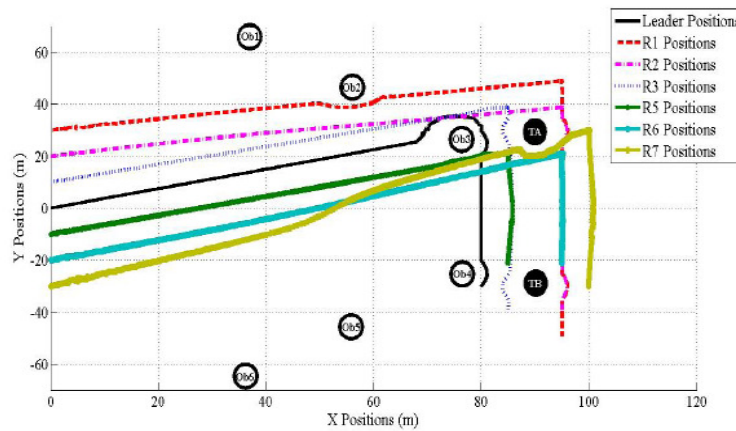


FIGURE 4: Sim(1) - Actual Path Trajectories

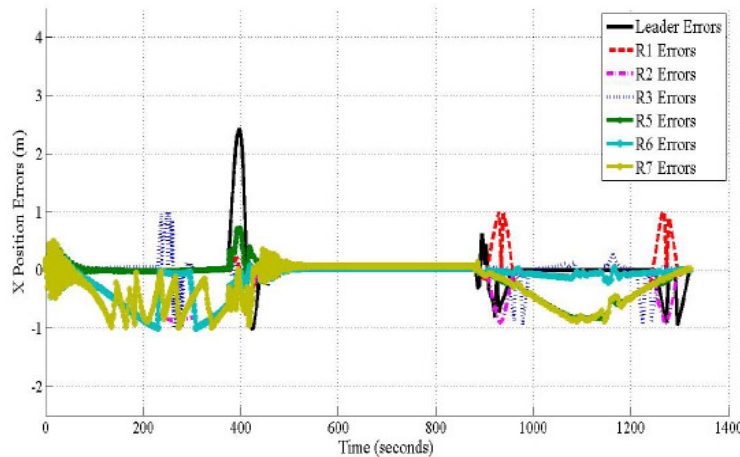
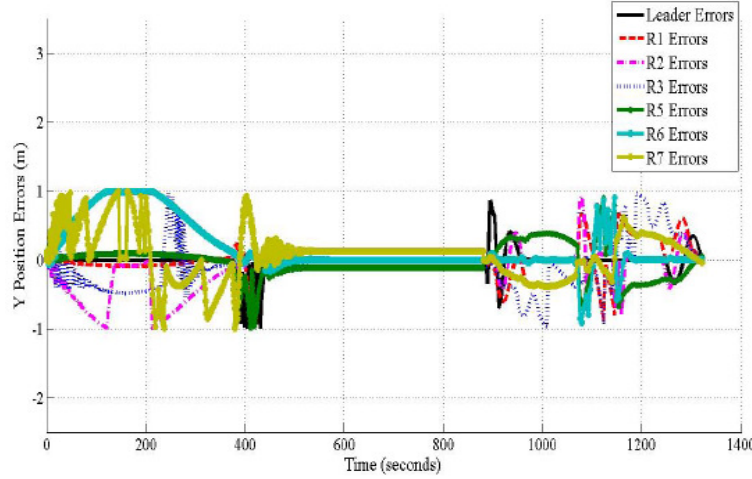


FIGURE 5: Sim(1) - Slave Positions Errors in the x-direction

**FIGURE 6: Sim(1) - Slave Positions Errors in the y-direction**

3.2 Simulation - Sim(2)

In Sim (2), the task, object capture for two targets, TA and TB, was executed by the subteams formed by the seven mobile robots. The seven robots, R1-7, could form 35 types of Robot Combos (Subteams (Sub1-35)) as shown in Table 3.

Subteam	Combo	Subteam	Combo	Subteam	Combo
Sub1	R1 R2 R3	Sub13	R1 R5 R6	Sub25	R2 R6 R7
Sub2	R1 R2 R4	Sub14	R1 R5 R7	Sub26	R3 R4 R5
Sub3	R1 R2 R5	Sub15	R1 R6 R7	Sub27	R3 R4 R6
Sub4	R1 R2 R6	Sub16	R2 R3 R4	Sub28	R3 R4 R7
Sub5	R1 R2 R7	Sub17	R2 R3 R5	Sub29	R3 R5 R6
Sub6	R1 R3 R4	Sub18	R2 R3 R6	Sub30	R3 R5 R7
Sub7	R1 R3 R5	Sub19	R2 R3 R7	Sub31	R3 R6 R7
Sub8	R1 R3 R6	Sub20	R2 R4 R5	Sub32	R4 R5 R6
Sub9	R1 R3 R7	Sub21	R2 R4 R6	Sub33	R4 R5 R7
Sub10	R1 R4 R5	Sub22	R2 R4 R7	Sub34	R4 R6 R7
Sub11	R1 R4 R6	Sub23	R2 R5 R6	Sub35	R5 R6 R7
Sub12	R1 R4 R7	Sub24	R2 R5 R7		

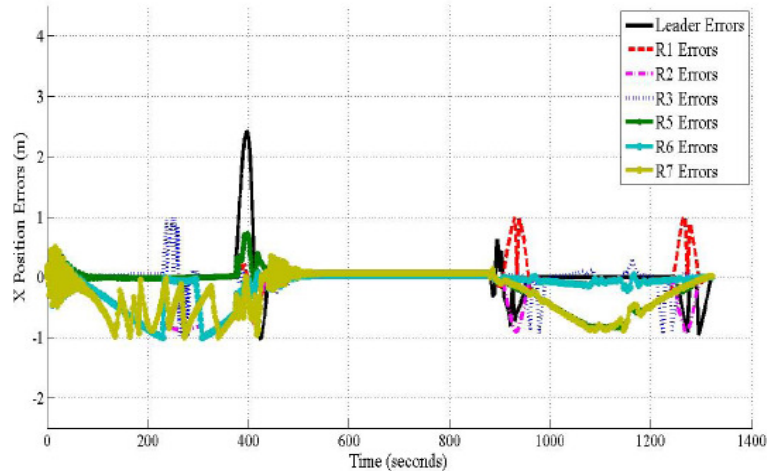
TABLE 3: Robot combinations (robot subteams)

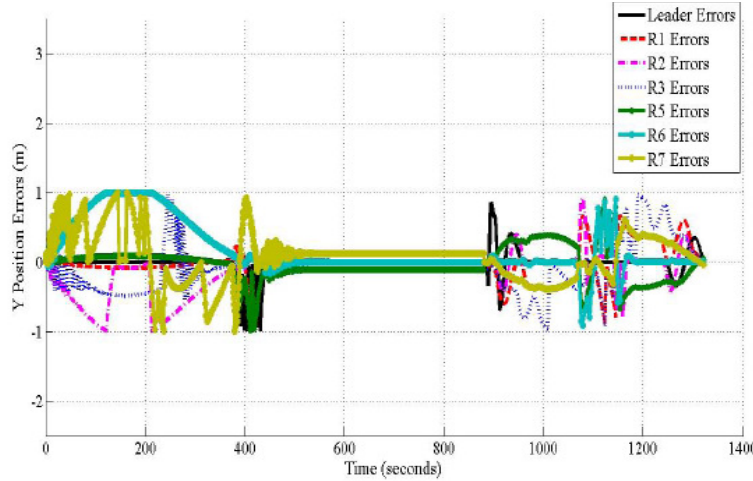
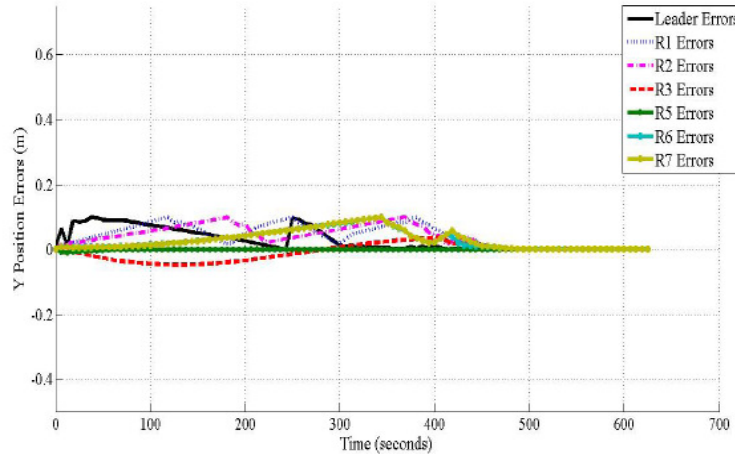
With the robot-target pairing method in Eqs (1) – (12), WAGT was generated. Subteams (Sub1 - 35) and their bids for the task were found for TA and TB in Table 4. Their bids were calculated in Eq. (9) as an inverse of the sum of robot-target distances in a subteam minus the base price when the base price for the task was 10. The reason was that in order to start with the tasks, the robots needed to maintain at least 10(m) from a target to capture it. The bids (T_a, T_b) in Table 4 were written where T_a was the bid values calculated for TA when T_b was the bid values calculated for TB.

Subteam	Bids	Subteam	Bids	Subteam	Bids
Sub1	(41,69)	Sub13	(39,73)	Sub25	(38,76)
Sub2	(40,69)	Sub14	(39,74)	Sub26	(39,74)
Sub3	(40,70)	Sub15	(38,75)	Sub27	(39,75)
Sub4	(40,71)	Sub16	(40,71)	Sub28	(39,75)
Sub5	(39,71)	Sub17	(40,71)	Sub29	(39,76)
Sub6	(40,70)	Sub18	(39,73)	Sub30	(38,76)
Sub7	(40,71)	Sub19	(39,73)	Sub31	(38,77)
Sub8	(40,72)	Sub20	(39,73)	Sub32	(38,77)
Sub9	(39,72)	Sub21	(39,74)	Sub33	(38,78)
Sub10	(40,72)	Sub22	(39,74)	Sub34	(38,78)
Sub11	(39,73)	Sub23	(39,75)	Sub35	(38,79)
Sub12	(39,73)	Sub24	(39,75)		

TABLE 4: Weighted Attack Guidance Table (WAGT) for Target A & B

As shown in Figure 7, only R4 was teleoperated by the human operator when all R1-3 and R5-7 automatically formed two subteams, (R1-3 and R5-7 combos) to capture TA and TB simultaneously in 625 seconds, respectively. However, R4 was not engaged in any task, which could reduce the time delay effect on the task achievements. All tasks were done by the two subteams, Sub1 and Sub35, fully autonomously. The position errors were from 0 to 0.12 (m) in Figures 8 and 9, and a position error average was 0.05 (m).

**FIGURE 7: Sim(2) - Actual Path Trajectories**

**FIGURE 8: Sim(2) - Slave Positions Errors in the x-direction****FIGURE 9: Sim(2) - Slave Positions Errors in the y-direction**

3.3 Discussions on Results

Pairing methods	Execution time(seconds)	Found subteam/target pairs
Swarm particle optimization (SPO) [32]	95.6	(Sub1 - TA) and (Sub35 - TB)
Market based method [13]	103.2	(Sub1 - TA) and (Sub35 - TB)
Genetic method [9]	110.3	(Sub1 - TA) and (Sub35 - TB)
Auction based method [39]	93.2	(Sub1 - TA) and (Sub35 - TB)
Sim (2)	90.2	(Sub1 - TA) and (Sub35 - TB)

TABLE 5: Performance comparison for robot-target pairing methods

By comparing those errors in Figures 8 and 9 and 5 and 6, the performance of the system in Sim (2) was better than that in Sim (1) when the simulations showed that in Sim (2), the task was finished more quickly, and the position errors were smaller. The reasons were (1) the amount of information transmitted over the time-varying links between the master and slave subsystems became less in Sim(2) than Sim(1) when only autonomous local slave robots in Sim (2) handled the task, but the teleoperated robot, the team leader, acted as a supervisor to monitor other robot

operations. (2) Forming the subteams could save all seven robots from visiting all targets to complete the task because the seven robots were split into three robots in a subteam to perform the task on different targets simultaneously as shown in Figure 7. By taking advantage of the task planning independently done by each subteam, the task completion was more effective when the operation time was decreased to 625 seconds in Sim(2) from 1350 seconds in Sim(1) in Figures 9 and 6, respectively, since the average speeds of the robots were equivalent during the simulations.

Besides, in the simulations, we implemented different pairing methods in Table 5 to the scenario mentioned above. As shown in the table, those pairing methods were run to compute various subteam-target pairs in different durations of time so called the execution time. In comparison with the data from other findings [9,13,32,39], the convergence rates with swarm particle optimization (SPO), auction based, and proposed pairing methods [32,39] were faster than those with the market and genetic methods [9,13] by 20-30 second execution time because the algorithms for SPO, auction based, and the proposed pairing methods are simpler. However, the algorithms for the SPO and auction based methods [32,39] are rigid; hence, they are inappropriate for target capturing if an obstacle is not known beforehand, but in fact, most of the working environments in engineering applications are uncertain. Therefore, only the proposed pairing method in Sim (2) can present the relatively fast and stable convergence to get robot-target pairs because of its simple algorithm. In addition, due to its flexibility, it is also applicable to target capturing even if no apriori knowledge about obstacles is available since no obstacle data is required to solve Eqs (1) – (12).

4. CONCLUSION & FUTURE WORK

The proposed control methods are developed for the SMMS mobile teleoperations to work on multi-targets and improve the performance in terms of the effectiveness of the task achievement and the system transparency as seen from the simulation results. In the simulations, the time required to complete the task by the slave robots was reduced from 1350 seconds in Sim (1) to 625 seconds in Sim (2). With the proposed robot-target pairing method, the robots made subteams that autonomously worked on paired targets in the modified potential field leader-follower formation, which makes the SMMS system be capable of handling multi-targets simultaneously in a short time. Moreover, by comparing the proposed robot-target pairing method to the others in [9,30,32,39], it is so simple that a relatively fast convergence rate to obtain an optimal solution (proper robot-target pairs) is achieved. Besides, the results also showed that the smaller position errors in Sim(2) than those in Sim(1) represents the transparency enhancement. The reason is the effect on the robotic system due to the time-varying communication delays is reduced because during the operation, with the proposed control methods, all slave robots except a team leader become completely autonomous. The team leader is the only robot teleoperated by the human operator in a team but not engaged in any task when the time-varying delays mostly happen over the long distance wireless communication between the master and slave team leader robots [28,27]. Therefore, it was shown that in Sim (2), task efficiency and conditional transparency were improved despite the fact that the system was subjected to the time-varying communication delay. Moreover, the slave robots with the proposed control methods can avoid obstacles and track and then capture targets when (1) the modified potential field based leader-follower formation and (2) the robot-target pairing method take effect. Nonetheless, the robot-target pairing method could only generate a suboptimal solution in general since it is based on some heuristic data that come from human experiences.

Therefore, our future work will be to further evaluate the performance of the MRMTMT pairing method and the performance and quality of the robot-target pair solutions. In addition, we will look into the proposed control method for a SMMS system working in very complex tasks and environments, e.g. a task that may require identification of positions and types of the uncertain targets in an unknown area. We will install the proposed control methods into SMMS system hardware for further experimental validation based on comparative studies on the results from experiments and simulations to emphasize the expected good performance achievement although the real time delays may vary irregularly.

5. REFERENCES

- [1] K. R. Baghæi and A. Agah. "task allocation methodologies for multi-robot systems", *Technical Report ITTC-FY2003-TR-20272-01*, 2003.
- [2] T. Balch and R.C. Arkin. "behavior-based formation control for multirobot teams", *Robotics and Automation, IEEE transactions*, 14(6):926-939, 1998.
- [3] L. Barnes, W. Alvis, M.A. Fields, K. Valavanis, and W. Moreno. "heterogeneous swarm formation control using bivariate normal functions to generate potential fields", *Distributed Intelligent Systems: Collective Intelligence and Its Applications, 2006. DIS 2006, IEEE Workshop*, pages 85-94, 2006.
- [4] Z. R. Bogdanowicz and N.P. Coleman. "new algorithm for optimization of effect-based weapon-target pairings", *International Conference Scientific Computing CSC 08*, 2008.
- [5] Y. Cheung. "Adaptive semi-autonomous teleoperation of a mutli-agent robotic system", *PhD thesis*, Stevens Institute of Technology, 2009.
- [6] Y. Cheung and J. Chung. "cooperative control of a multi-arm system using semi-autonomous telemanipulation and adaptive impedance", *14th IEEE International Conference on Advanced Robotics (ICAR)*, 2009.
- [7] Y. Cheung, J.H. Chung, and N. Coleman, "semi-autonomous formation control of a single-master multi-slave teleoperation system", *IEEE Symposium on Computational Intelligence in Control and Automation*, 2009.
- [8] S. Cifuentes, J.M. Giron-Sierra, and J.F. Jimenez, "robot formation control based on a multi-potential approach", *Control Automation and Systems (ICCAS), 2010 International Conference*, pages 1982-1987, 2010.
- [9] L. Delin, S. Chunlin, W. Biao, and W. Wenhai, "air combat decision-making for cooperative multiple target attack using heuristic adaptive genetic algorithm", *Machine Learning and Cybernetics, Proceeding of 2005 International Conference*, (1)473-478, 2005.
- [10] L. Delin, D. Haibin, W. Shunxiang, and L. Maoqing, "research on air combat decision-making for cooperative multiple target attack using heuristic ant colony algorithm", *ACTA AERONAUTICA ET ASTRONAUTICA SINICA*, 27(6) pages 1166-1170, 2006.
- [11] L. Delin, Y. Zhong, D. Haibin, W. Zaogui, and S. Chunlin, "heuristic particle swarm optimization algorithm for air combat decision-making on CMTA", *Transactions of Nanjing University of Aeronautics and Astronautics*, 23(1) pages. 20-26, 2006.
- [12] J.P. Desai, J.P. Ostrowski, and V. Kumar, "modeling and control of formations of non-holonomic mobile robots", *Robotics and Autonmation, IEEE Transactions*, 17(6) pages. 905-908, 2001.
- [13] M.B. Dias, R.M. Zlot, N. Kalra, and A. Stentz, "market-based multirobot coordination: a survey and analysis", *Proceedings of the IEEE*, 94(7) pages. 1257-1270, 2006.
- [14] K.D. Do, "formation control of mobile agents using local potential functions", *American Control Conference*, 2006.

- [15] M. Eghbali and M.A. Sharbafi, "multi-agent routing to multi-targets via ant colony", *Computer and Automation Engineering (ICCAE), 2010 the 2nd International Conference*, (1)pages. 587-591, 2010.
- [16] P.G. Espejo, S. Ventura, and F. Herrera, "a survey on the application of genetic programming to classification", *Systems, Man., and Cybernetics, Part C: Applications and Reviews, IEEE Transactions*, 40(2), pages. 121-144, 2010.
- [17] I. Farkhatdinov and J.H. Ryu, "teleoperation of multi-robot and multi-property systems", *Industrial Informatics, INDIN 2008, 6th IEEE International Conference*, pages 1453-1458, 2008.
- [18] T. Fong, C. Thorpe, and C. Baur, "multi-robot remote driving with collaborative control", *Industrial Electronics, IEEE Transactions*, 50(4) pages. 699-704, 2003.
- [19] D. Fox, W. Burgard, H. Kruppa, and S. Thrun, "collaborative multi-robot localization", *In Proceedings of the German Conference on Artificial Intelligence and the 21st Symposium on Pattern Recognition*, 1999.
- [20] S.S. Ge, C.H. Fua, and W.M. Liew, "swarm formations using the general formation potential function", *Robotics, Automation, and Mechatronics, 2004 IEEE Conference*, (2) pages. 655-660, 2004.
- [21] J.P. Graciano, "a simple navigation algorithm with no local minima", *Advanced Robotics, ICAR 2005, Proceedings, 12th International Conference*, pages 640-646, 2005.
- [22] K. Hashtrudi-Zaad and S.E. Salcudean, "adaptive transparent impedance reflecting teleoperation", *Proceeding of the 1996 IEEE International Conference on Robotics and Automation*, 1996.
- [23] B. Kaleci, O. Parlaktuna, M. Ozkan, and G. Kirlik, "market-based task allocation by using assignment problem", *Systems, Man, and Cybernetics (SMC), 2010, IEEE International Conference*, pages 135-141, 2010.
- [24] M.T. Khan, T. Immanuel, and C.W. DeSilva, "autonomous market-based multi-robot cooperation", *Intelligent and Advanced Systems (ICIAS), 2010 International Conference*, pages 1-6, 2010.
- [25] W. Kim, D.S. Cho, and H.J. Kim, "sequential multi-agent task assignment using auction algorithm based on d*lite", *Control Automation and Systems (ICCAS), 2010 International Conference*, page 938-942, 2010.
- [26] E. Lalish, K.A. Morgansen, and T. Tsukamaki, "formation tracking control using virtual structures and deconfliction", *Decision and Control, 2006, 45th IEEE Conference*, pages 5699-5705, 2006.
- [27] D. Lee, O. Martinez-Palafox, and M.W. Spong, "bilateral teleoperation of multiple cooperative robots over delayed communication networks: Theory", *Robotics and Automation, ICRA, Proceedings of the IEEE International Conference*, 2005.
- [28] D. Lee and M.W. Spong, "bilateral teleoperation of multiple cooperative robots over delayed communication networks: Application", *Robotics and Automation, ICRA Proceedings of the 2005 IEEE International Conference*, 2005.
- [29] H.K. Lee, M.H. Shin, and M.J. Chung, "adaptive controller of master-slave systems for transparent teleoperation", *ICAR 1997*, pages 14-23, 1997.

- [30] Z.J. Lee, C.Y. Lee, and S.F. Su, "an immunity-based ant colony optimization algorithm for solving weapon target assignment problem", *Applied Soft Computing Journal*, 2(1) pages. 39-47, 2002.
- [31] C.S. Lim, R. Mamat, and T. Braunl, "market-based approach for multi-team robot cooperation", *Autonomous Robots and Agents, 2009, ICARA 2009, 4th International Conference*, pages 62-67, 2009.
- [32] B. Liu, Z. Qin, R. Wang, Y.B. Gao, and L.P. Shao, "a hybrid heuristic particle swarm optimization for coordinated multi-target assignment", *Industrial Electronics and Applications, ICIEA, 4th IEEE Conference*, pages 1929-1934, 2009.
- [33] J. Liu, L. Shun, T. Chen, X. Huang, and C. Zhao, "competitive multi-robot teleoperation", *Robotics and Automation, 2005, ICRA 2005, Proceedings of the 2005 IEEE International Conference*, pages 75-80, 1993.
- [34] K.F. Man, F.S. Tang, and S. Kwong, "genetic algorithms: concepts and applications in engineering designs", *Industrial Electronics, IEEE Transactions*, 43(5) pages. 519-534, 1996.
- [35] S. Monteiro and E. Bicho, "robots allocation and leader-follower pairs", *Robotics and Automation, ICRA, IEEE International Conference*, pages 3769-3775, 2008.
- [36] J. Ota, N. Miyata, T. Arai, E. Yoshida, D. Kurabatashi, and J. Sasaki, "transferring and regrasping a large object by cooperation of multiple mobile robots", *Human Robot Interaction and Cooperative Robots, Proceedings of IEEE/RSJ International Conference*, 1995.
- [37] H. Park, Y.A. Lim, A. Pervez, B.C. Lee, S.G. Lee, and J. Ryu, "teleoperation of a multi-purpose robot over the internet using augmented reality", *Control, Automation, and Systems, 2007, ICCAS 2007, International Conference*, pages 2456-2461, 2007.
- [38] M.G. Park and M.C. Lee, "real-time path planning in unknown environment and a virtual hill concept to escape local minima", *Industrial Electronics Society, 2004, IECON 2004, 30th Annual Conference of IEEE*, (3) pages.2223 – 2228, 2004.
- [39] A. Pongpunwattana and R. Rysdyk, "real-time planning for multiple autonomous vehicles in dynamic uncertain environments", *Journal of Aerospace Computing, Information, and Communication*, 1(12) pages. 580-604, 2004.
- [40] J.H. Ryu, D.S. Kwon, and B. Hannaford, "stable teleoperation with time-domain passivity control", *Robotics and Automation, IEEE Transactions*, 20(2) pages. 365-373, 2004.
- [41] C. Sabattini, C. Secchi, and C. Fantuzzi, "potential based control strategy for arbitrary shape formations of mobile robots", *Intelligent Robots and Systems, 2009, IROS 2009, IEEE/RSJ International Conference*, pages 3762-3767, 2009.
- [42] T. Suzuki, T. Sekine, T. Fujii, H. Asama, and I. Endo, "cooperative formation among multiple mobile robot teleoperation in inspection task", *Decision and Control 2000, Proceedings of the 39th IEEE Conference*, 1(12-15), pages. 358-363, 2000.
- [43] H. Tan, Q. Liao, and J. Zhang, "an improved algorithm of multiple robot cooperation in obstacle existing environment", *Robotics and Biomimetics, 2007, ROBIO 2007*, pages 1001-1006, 2007.

- [44] L.M. Wachter and L.E. Ray, "stability of potential function formation control with communication and processing delay", *American Control Conference, 2009, ACC 2009*, pages 2997-3004, 2009.
- [45] Z. Wang, M.N. Admadabadi, E. Nakano, and T. Takahashi, "a multiple robot system for cooperative object transportation with various requirements on task performing", *Robotics and Automation, 1999, Proceedings of 1999 IEEE International Conference*, 2(10-15) pages 1226-1233, 1999.
- [46] H. Yamaguchi, "a distributed motion coordination strategy for multiple nonholonomic mobile robots in cooperative hunting operations", *Decision and Control, 2002, Proceedings of the 41st IEEE Conference*, 3(10-13) pages 2984-2991, 2002.
- [47] Y. Yamamoto and S. Fukuda, "trajectory planning of multiple mobile manipulators with collision avoidance capability", *Proceedings of ICRA 2002 IEEE International Conference*, 2002.
- [48] Z. Yao and K. Gupta, "distributed strategies for local minima escape in motion planning for mobile networks", *Robot Communication and Coordination, 2009, ROBO-COMM 2009, Second International Conference*, pages 1-7, 2009.